Supplemental Material for: Non-Hermitian Waveguide Cavity QED with Tunable Atomic Mirrors

Wei Nie,[1,*] Tao Shi,[2,3] Yu-xi Liu,[4] and Franco Nori[5,6,7]

[1] *Center for Joint Quantum Studies and Department of Physics, School of Science, Tianjin University, Tianjin 300350, China*
[2] *Institute of Theoretical Physics, Chinese Academy of Sciences, P.O. Box 2735, Beijing 100190, China*
[3] *CAS Center for Excellence in Topological Quantum Computation, University of Chinese Academy of Sciences, Beijing 100049, China*
[4] *School of Integrated Circuits, Tsinghua University, Beijing 100084, China*
[5] *Theoretical Quantum Physics Laboratory, Cluster for Pioneering Research, RIKEN, Wakoshi, Saitama 351-0198, Japan*
[6] *Center for Quantum Computing, RIKEN, Wakoshi, Saitama 351-0198, Japan*
[7] *Physics Department, The University of Michigan, Ann Arbor, Michigan 48109-1040, USA*

In the Supplemental Material, we present the details about the main results in this work.

I. QUANTUM MIRROR WITH CONTROLLABLE REFLECTION

The tunable reflection of mirrors can be used for manipulating cavities. The atomic mirrors studied in previous works rely on waveguide-induced collective quantum effects to enhance light reflection. For these atomic mirrors without direct couplings between atoms, it is challenging to tune the reflection of light. In this section, we discuss the difference between Bragg and anti-Bragg conditions in affecting the reflection of light from two coupled atoms in a waveguide. In particular, we show the advantages of the direct coupling between the atoms in order to manipulate mirror reflection.

A. Waveguide scattering theory and tunable quantum interference in photon reflection

Waveguides are an important interface for light-matter interaction. Photons propagating in a waveguide can be scattered by a single atom or an atom array. Without loss of generality, we consider that the atom-waveguide interaction is much weaker compared to atomic frequency ω_0. In the Born-Markov approximation, the atom-waveguide coupled quantum system can be described by a master equation ($\hbar = 1$)

$$\dot{\rho}(t) = -i[H_0 + H_{\mathrm{w}}, \rho(t)] + \mathcal{D}[\rho]. \tag{S1}$$

Here, H_0 is the Hamiltonian of the atomic system, and H_{w} denotes long-range atom-atom interactions induced by the waveguide, i.e., $H_{\mathrm{w}} = \sum_{ij} g_{ij}(\sigma_i^+\sigma_j^- + \mathrm{H.c.})$, where g_{ij} are related to decay rates of atoms. Operators of atoms are $\sigma_i^+ = |e_i\rangle\langle g_i|$ and $\sigma_i^- = |g_i\rangle\langle e_i|$, where $|g_i\rangle$ and $|e_i\rangle$ are the ground state and excited state of the ith atom, respectively. Obviously, interactions in H_{w} are coherent. In addition to coherent atom-atom interactions, continuous photonic modes in the waveguide give rise to correlated dissipation between atoms. This is described by the Lindblad operator

$$\mathcal{D}[\rho] = \sum_{i,j} \gamma_{ij} \left(2\sigma_i^-\rho\sigma_j^+ - \sigma_i^+\sigma_j^-\rho - \rho\sigma_i^+\sigma_j^-\right). \tag{S2}$$

In the literature, γ_{ij} are also known as dissipative couplings. These are responsible for collective quantum effects, e.g., superradiance and subradiance. In a one-dimensional waveguide, one can show that the coherent couplings and dissipative couplings are

$$g_{ij} = \sqrt{\Gamma_i\Gamma_j}\sin\left(\frac{2\pi d_{ij}}{\lambda_0}\right), \tag{S3}$$

$$\gamma_{ij} = \sqrt{\Gamma_i\Gamma_j}\cos\left(\frac{2\pi d_{ij}}{\lambda_0}\right), \tag{S4}$$

* weinie@tju.edu.cn

respectively. Here, Γ_i denotes the waveguide-induced decay rate of the ith atom. Without loss of generality, we assume that atoms coupled to the waveguide have the same decay rate Γ. Above, d_{ij} is the spacing between the ith and jth atoms, and λ_0 is the wavelength of the photons corresponding to atomic frequency ω_0. The single-photon reflection amplitude in the waveguide is [S1]

$$r = -i\Gamma \sum_{i,j} G_{ij} \exp[ik_0(x_i + x_j)], \tag{S5}$$

with $k_0 = \omega_0/c$, and G_{ij} are matrix elements of the Green's function

$$G = \frac{1}{\omega - H_{\text{eff}}}. \tag{S6}$$

Here, ω is the frequency of the driving field in the waveguide. Eq. (S5) can be written as

$$r = -i\Gamma \boldsymbol{V}^\top \frac{1}{\omega - H_{\text{eff}}} \boldsymbol{V}, \tag{S7}$$

where the vector $\boldsymbol{V} = (e^{ik_0x_1}, e^{ik_0x_2}, \cdots)^\top$ represents propagating photons in the waveguide. H_{eff} is the non-Hermitian effective Hamiltonian of the atom-waveguide system

$$H_{\text{eff}} = H_0 + H_{\text{w}} - i \sum_{ij} \gamma_{ij} (\sigma_i^+ \sigma_j^- + \text{H.c.}). \tag{S8}$$

Therefore, optical responses in the waveguide are determined by this effective Hamiltonian. For simplicity, we diagonalize the effective Hamiltonian as $H_{\text{eff}} = \sum_j E_j |\Phi_j^R\rangle\langle\Phi_j^L|$, with the biorthogonal basis $\langle\Phi_j^L|\Phi_{j'}^R\rangle = \delta_{jj'}$. In terms of the eigenvectors of the effective Hamiltonian, the reflection amplitude becomes

$$r(\omega) = -i\Gamma \sum_j \frac{\boldsymbol{V}^\top |\Phi_j^R\rangle\langle\Phi_j^L| \boldsymbol{V}}{\omega - \text{Re}(E_j) - i\text{Im}(E_j)} \tag{S9}$$

Here, x_i denotes the position of the ith atom in the waveguide. Equation (S9) shows that photon reflection in the waveguide results from quantum interference between scattered photons. Specifically, photon reflection is related to energies and decay rates of the eigenstates, as well as the interaction spectrum $\boldsymbol{V}^\top |\Phi_j^R\rangle\langle\Phi_j^L| \boldsymbol{V}$ in the reflection process [S2].

From Eqs. (S3) and (S4), we know that atomic spacing determines the waveguide-mediated couplings. Therefore, scattering states in the atomic system are changed by the atomic spacing, giving rise to various interaction spectra. We discuss two types of atomic spacings, which have distinct influences on the reflection of light.

B. Bragg atomic mirror

The Bragg scattering condition is defined by the atomic spacing $d = n\lambda_0/4$, where n is an even number. In this scenario, atoms in the waveguide have largest dissipative couplings. However, the coherent coupling is

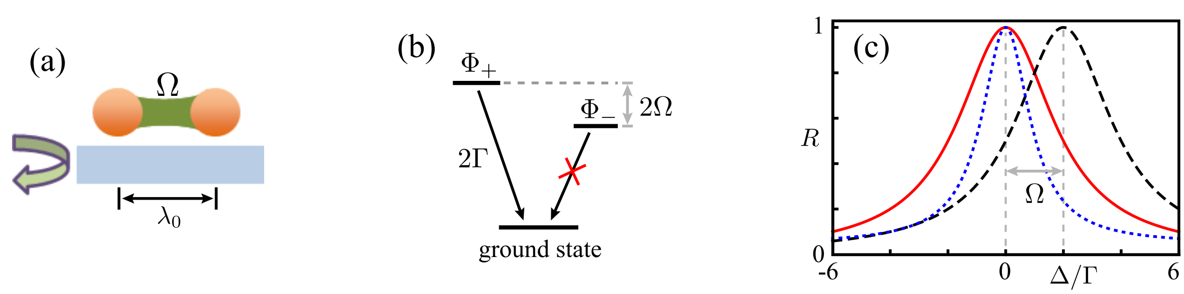

FIG. S1. (a) Schematic diagram of a Bragg atom-dimer mirror in a waveguide. (b) V-type energy levels of the atom dimer. The superradiant state has decay rate 2Γ, and the dark state does not decay. (c) Reflection of the Bragg atom-dimer mirror. Red-solid and black-dashed curves correspond to Bragg atom-dimer mirrors with $\Omega = 0$ and $\Omega = 2\Gamma$, respectively. The blue-dotted curve denotes the refection of a single atom.

vanishing. Therefore, atoms have strong cooperative light-matter interactions, producing collective quantum effects, e.g., superradiance and subradiance. In waveguide QED, Bragg scattering is of considerable interest in studying photon transport. Waveguide-induced superradiant states enhance light reflection. Therefore, high-finesse atomic cavities can be realized [S3].

We consider an atom dimer coupled to a waveguide, as shown in Fig. S1(a). Two atoms have a direct coupling Ω. The corresponding Hamiltonian is $H_0 = \omega_0(\sigma_1^+\sigma_1^- + \sigma_2^+\sigma_2^-) + \Omega(\sigma_1^+\sigma_2^- + \text{H.c.})$. In the Bragg condition with atomic spacing $d = \lambda_0$, we have $g_{12} = 0$ and $\gamma_{12} = i\Gamma$. Therefore, the effective Hamiltonian of two coupled atoms is

$$H_{\text{eff,Bragg}} = \begin{pmatrix} \omega_0 - i\Gamma & \Omega - i\Gamma \\ \Omega - i\Gamma & \omega_0 - i\Gamma \end{pmatrix}. \tag{S10}$$

We can obtain the eigenenergies

$$E_\pm = \omega_0 - i\Gamma \pm (\Omega - i\Gamma). \tag{S11}$$

Namely, $E_+ = \omega_0 + \Omega - i2\Gamma$ and $E_- = \omega_0 - \Omega$. The corresponding eigenstates are symmetric and anti-symmetric superpositions of two mirror atoms, i.e., $|\Phi_+\rangle = \frac{1}{\sqrt{2}}(1,1)^\top$ and $|\Phi_-\rangle = \frac{1}{\sqrt{2}}(1,-1)^\top$, respectively.

Energy levels of the Bragg atom-dimer mirror are shown in Fig. S1(b). In particular, $|\Phi_+\rangle$ is a superradiant state with a decay rate 2Γ, and $|\Phi_-\rangle$ is the subradiant state without dissipation. The atomic coupling Ω changes the energy splitting between these two collective states. One can find the interaction spectrum $\boldsymbol{V}^\top|\Phi_+^R\rangle\langle\Phi_+^L|\boldsymbol{V} = 2$ for the superradiant state $|\Phi_+\rangle$. Because $|\Phi_-\rangle$ is a dark state, its interaction spectrum is $\boldsymbol{V}^\top|\Phi_-^R\rangle\langle\Phi_-^L|\boldsymbol{V} = 0$. Therefore, the reflection amplitude of the Bragg atom dimer becomes

$$r(\Delta) = \frac{-i2\Gamma}{\Delta - \Omega + i2\Gamma}, \tag{S12}$$

with $\Delta = \omega - \omega_0$. The reflection spectrum is shown in Fig. S1(c). The atomic coupling gives rise to a shift of the reflection spectrum with respective to the one $\Omega = 0$. Although the spectrum is broader, the profile is still Lorentzian. The reflection spectrum of this Bragg atom dimer is the same as for a single atom with frequency $\omega_0 + \Omega$ and decay rate 2Γ. In other words, the atomic coupling plays a trivial role in changing the reflection spectrum of a Bragg atom dimer.

C. Anti-Bragg atomic mirror

Distinct from the Bragg atomic mirror, the anti-Bragg atom-dimer mirror produces a single-peak or two-peak reflection spectrum depending on the direct atomic coupling Ω. This reflection-tunable mirror makes it possible to control the flow of light in the waveguide. The anti-Bragg condition is defined by the atomic spacing $d = m\lambda_0/4$, where m is an odd number. Without loss of generality, the spacing between two atoms is assumed to be $d = \lambda_0/4$. In this scenario, the waveguide induces the coherent coupling between the two atoms; however, the dissipative coupling is vanishing. Therefore, the non-Hermitian Hamiltonian of the waveguide-mediated atom-dimer mirror is

$$H_{\text{eff,anti}-\text{Bragg}} = \begin{pmatrix} \omega_0 - i\Gamma & \Omega + \Gamma \\ \Omega + \Gamma & \omega_0 - i\Gamma \end{pmatrix}. \tag{S13}$$

The eigenvalues of the Hamiltonian in Eq. (S13) are $E_\pm = \omega_0 \pm (\Omega + \Gamma) - i\Gamma$. The eigenvectors are $|\Phi_+\rangle = \frac{1}{\sqrt{2}}(1,1)^\top$ and $|\Phi_-\rangle = \frac{1}{\sqrt{2}}(1,-1)^\top$, same as for the Bragg atom dimer. Different from the Bragg counterpart, the anti-Bragg atom dimer has two scattering states with the same decay rate. Therefore, both of them are responsible for reflection of light in the waveguide. Another difference from the Bragg atom dimer is that no collective quantum effect appears in the anti-Bragg atom dimer. In this sense, the anti-Bragg atom mirror seems to be trivial. In fact, the anti-Bragg condition gives rise to many interesting optical properties in the atom-dimer mirror.

From the multi-channel scattering approach [S2], the reflection amplitude produced by the anti-Bragg atom-dimer mirror is

$$r(\Delta) = -i\Gamma\left(\frac{\boldsymbol{V}^\top|\Phi_+^R\rangle\langle\Phi_+^L|\boldsymbol{V}}{\Delta - (\Omega + \Gamma) + i\Gamma} + \frac{\boldsymbol{V}^\top|\Phi_-^R\rangle\langle\Phi_-^L|\boldsymbol{V}}{\Delta + (\Omega + \Gamma) + i\Gamma}\right). \tag{S14}$$

These two scattering states have different energies $\omega_0 \pm (\Omega + \Gamma)$. Different from the Bragg atom-dimer mirror, the anti-Bragg atom-dimer mirror yields quantum interference in the reflection process. After a straightforward

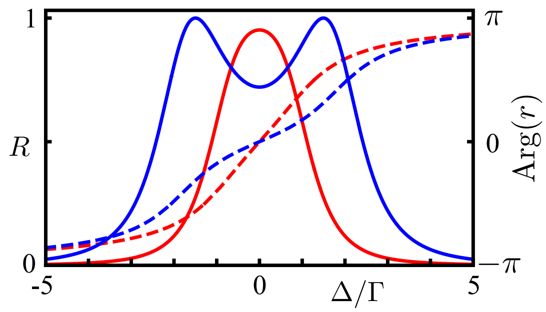

FIG. S2. Reflection intensity $R = |r|^2$ (solid) and photon phase shift $\mathrm{Arg}(r)$ (dashed) produced by the anti-Bragg atomic mirror. Red and blue curves correspond to $\Omega = -0.2\Gamma$ and $\Omega = 0.6\Gamma$, respectively. The phase shift at $\Delta = 0$ is zero for the single-peak and two-peak reflection spectra.

calculation, we obtain the interaction spectra between propagating photons in the waveguide and atom-dimer mirror: $\boldsymbol{V}^\top|\Phi_+^R\rangle\langle\Phi_+^L|\boldsymbol{V} = -i$, and $\boldsymbol{V}^\top|\Phi_-^R\rangle\langle\Phi_-^L|\boldsymbol{V} = i$. Hence, the reflection intensity ($R = |r|^2$) becomes

$$R(\Delta) = \left|\left(\frac{-\Gamma}{\Delta - (\Omega+\Gamma) + i\Gamma} + \frac{\Gamma}{\Delta + (\Omega+\Gamma) + i\Gamma}\right)\right|^2. \tag{S15}$$

Quantum interference in the reflection process can be tuned by the atomic coupling Ω. By changing the energy difference $W = 2(\Omega+\Gamma)$ between two scattering states, the reflection of the atom-dimer mirror can be modified. Specifically, for $-\Gamma < \Omega \leq \Gamma$, the atom-dimer mirror yields a single-peak reflection spectrum. However, for $\Omega > \Gamma$, a two-peak reflection spectrum is obtained. In Fig. S2, we show the reflection intensities and phase shifts of photons for $\Omega = -0.2\Gamma$ and $\Omega = 0.6\Gamma$, respectively. For the reflection at the central frequency $\Delta = 0$, the phase shift is zero when $\Omega > -\Gamma$, different from the π phase shift in the light reflection produced by the Bragg atomic mirror. However, when two scattering states are swapped with $\Omega < -\Gamma$, a π phase shift is obtained.

We note that a waveguide-mediated anti-Bragg atom dimer with fixed direct coupling $\Omega = -\Gamma$ was recently realized in superconducting quantum circuits [S4]. We find that the atom dimer with $\Omega = -\Gamma$ gives rise to degenerate scattering states. Destructive quantum interference produces vanishing reflection for various frequencies. In other words, the atom-dimer mirror is transparent for incident photons. Hence, by tuning the atomic coupling Ω of the anti-Bragg atom-dimer mirror, we can drastically modify the reflection spectrum. This makes it feasible to realize a controllable open cavity using atomic mirrors, which is challenging for conventional optical cavities.

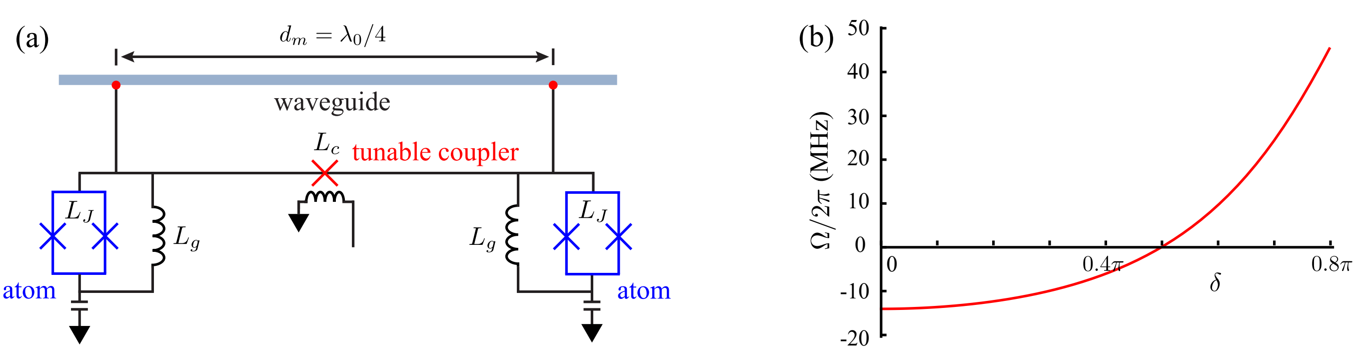

FIG. S3. (a) Schematic of anti-Bragg atom-dimer mirror in superconducting quantum circuits. The crosses represent Josephson junctions. Here, a superconducting artificial atom consists of two Josephson junctions. The tunable coupling between two artificial atoms can be realized by a Josephson junction. Two red dots denote coupling points between two atoms and the waveguide. (b) Tunable atomic coupling Ω versus δ, the phase difference across the coupler junction. Here, we consider $L_J = 8.34$ nH, $L_g = 0.2$ nH and $L_c = 0.566$ nH, as studied in the experiment [S5].

D. Tunable atomic coupling in superconducting quantum circuits

To realize the tunable atom-dimer mirror, we need to manipulate the direct coupling Ω between atoms. Waveguide QED with an atom dimer has been experimentally realized for fixed direct coupling between atoms [S4]. In this experiment, the direct coupling Ω is set to be $-\Gamma$, such that the coupling between the two atoms is zero. Here, we suggest an experimental setup for a tunable atom-dimer mirror, as shown in Fig. S3(a). A superconducting artificial atom consisting of two Josephson junctions is known as a gmon qubit. The coupling between two artificial atoms is mediated by a tunable Josephson junction with inductance L_c. Its concrete form is

$$\Omega = -\frac{M}{2}\frac{\omega_0}{L_J + L_g}, \tag{S16}$$

where the mutual inductance $M = L_g^2/(2L_g + L_c)$. Here, ω_0 is the frequency of two atoms. The Josephson inductance is $L_c = \Phi_0/(2\pi I_0 \cos\delta) = L_0/\cos\delta$, where $\Phi_0 = h/2e$ is the magnetic flux quantum; I_0 is the critical current of the coupler junction; and δ is the phase difference across the coupler junction. This phase difference can be controlled by the external dc flux. Therefore, the atom-atom coupling becomes

$$\Omega = -\frac{\omega_0}{2}\frac{L_g^2}{(L_J + L_g)(2L_g + \frac{L_0}{\cos\delta})}. \tag{S17}$$

This direct coupling can be tuned from positive to negative by controlling the phase δ of the coupler junction, as shown in Fig. S3(b). Here, we use the experimental parameters in Ref. [S5]. The atom-atom coupling can be appropriately adjusted by optimizing parameters of the circuit elements.

II. ATOMIC CAVITY PROTECTED BY ANTI-$\mathcal{PT}$ SYMMETRY

A waveguide has continuous photonic modes, which enable the propagation of light with various frequencies. The tunable reflection of mirror allows to control the flow of light in a waveguide. From this aspect, an atom dimer is more useful than a single atom. It has been shown [S6] that a large reflection of single-peak mirrors leads to an effective cavity mode. However, it is unclear how the effective cavity mode survives in an open atomic cavity with reduced mirror reflection. A controllable atomic coupling makes it possible to construct a reconfigurable cavity with atom-dimer mirrors. Such a cavity can be used to control light-matter interactions and has potential applications in quantum information processing. In this section, we discuss the mechanism of the atom-dimer cavity.

A. Cavity supermodes

For a cavity with tunable reflection, a challenge is how to build a connection between the properties of the cavity and the reflection of mirrors. We have shown in Sec. I that mirror reflection is related to the non-Hermitian Hamiltonian of the atom dimer. The reflection of light between two mirrors should be responsible for optical properties of an atomic cavity, which can be also described by a non-Hermitian Hamiltonian. In this way, we can understand how tunable mirror reflection nontrivially alters the cavity. We now consider a cavity consisting of two anti-Bragg atom-dimer mirrors with a separation λ_0 in the waveguide, as shown in Fig. S4(a). From Eqs. (S3) and (S4), the Hamiltonian of this system becomes

$$H_{\rm c} = -i\Gamma\sum_{j=1}^{4}\sigma_j^+\sigma_j^- + (\Omega+\Gamma)(\sigma_1^+\sigma_2^- + \sigma_3^+\sigma_4^- + \text{H.c.}) + \Gamma(\sigma_1^+\sigma_3^- + \sigma_1^+\sigma_4^- + \text{H.c.}) + i\Gamma(\sigma_1^+\sigma_4^- - \sigma_2^+\sigma_3^- + \text{H.c.}). \tag{S18}$$

To uncover the mirror-cavity relation, we write the non-Hermitian Hamiltonian of the atom-dimer cavity in the single-excitation subspace $\{\sigma_j^+|g_1g_2g_3g_4\rangle\}$ as

$$H_{\rm c} = \begin{pmatrix} -i\Gamma & \Omega+\Gamma & \Gamma & i\Gamma \\ \Omega+\Gamma & -i\Gamma & -i\Gamma & \Gamma \\ \Gamma & -i\Gamma & -i\Gamma & \Omega+\Gamma \\ i\Gamma & \Gamma & \Omega+\Gamma & -i\Gamma \end{pmatrix}. \tag{S19}$$

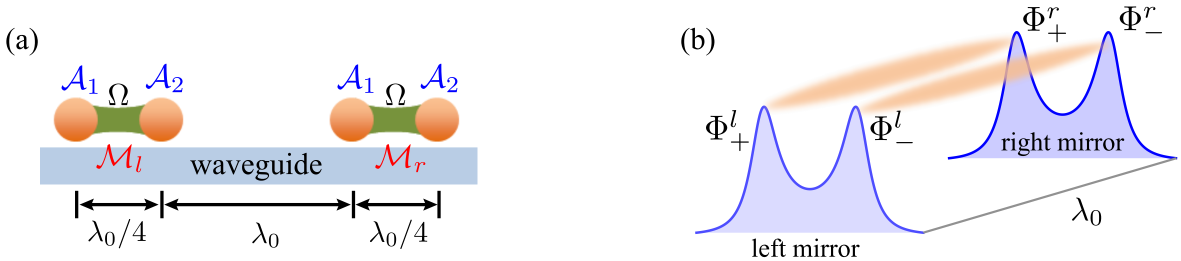

FIG. S4. (a) Schematics of a cavity with two anti-Bragg atom-dimer mirrors in a waveguide. The left and right mirrors are denoted by $\mathcal{M}_l$ and $\mathcal{M}_r$, respectively. In each mirror, there are two mirror atoms $\mathcal{A}_1$ and $\mathcal{A}_2$. The distance between two mirrors is $d = \lambda_0$. (b) Reflection spectra for two atom-dimer mirrors. Two peaks correspond to reflection channels in the atomic cavity.

In particular, two 2×2 matrices in the diagonal line denote the Hamiltonians of two mirrors. The other two matrices in the off-diagonal line are mirror-mirror couplings mediated by the waveguide. In subspaces of two mirrors and two mirror atoms, the Hamiltonian becomes

$$H_{\rm c} = (\Omega+\Gamma)s_0\otimes\tau_x + \Gamma s_x\otimes\tau_0 - i\Gamma s_y\otimes\tau_y - i\Gamma s_0\otimes\tau_0, \tag{S20}$$

i.e., Eq. (3) in the main text. Here, s_n and τ_n $(n = x, y, z)$ are Pauli matrices in the space $\{\mathcal{M}_l, \mathcal{M}_r\}$ of two mirrors and the subspace $\{\mathcal{A}_1, \mathcal{A}_2\}$ of mirror atoms, respectively. Equation (S20) characterizes the relation between the atomic cavity and mirrors. The first and the last terms represent the atomic coupling and decay rate of two atom-dimer mirrors, as we studied in Eq. (S13). The second and third terms describe the waveguide-induced dispersive and dissipative couplings between mirrors. Hence, the mode loss and distribution are determined by the interplay among the first three terms.

For the cavity with single-peak mirrors using single atoms [S6], an effective cavity mode is obtained with the anti-symmetric superposition of these two mirror atoms. Similarly, for the cavity with two-peak atomic mirrors, we may assume that there are two channels supporting cavity modes, as shown in Fig. S4(b). We consider superpositions of mirror states $\Phi_+^{\pm} = (1/\sqrt{2})(\Phi_+^l \pm \Phi_+^r)$ and $\Phi_-^{\pm} = (1/\sqrt{2})(\Phi_-^l \pm \Phi_-^r)$, where the indexes l and r denote the left and right mirrors, respectively. This is equivalent to making a unitary transformation

$$U = \begin{pmatrix} 1 & -1 & 1 & -1 \\ 1 & 1 & -1 & -1 \\ 1 & -1 & -1 & 1 \\ 1 & 1 & 1 & 1 \end{pmatrix}, \tag{S21}$$

to the atom-dimer cavity. We obtain the Hamiltonian

$$\begin{aligned} H_{\rm c} &= \begin{pmatrix} -\Omega - i\Gamma & -i\Gamma & 0 & 0 \\ -i\Gamma & \Omega - i\Gamma & 0 & 0 \\ 0 & 0 & -\Omega - 2\Gamma - i\Gamma & i\Gamma \\ 0 & 0 & i\Gamma & \Omega + 2\Gamma - i\Gamma \end{pmatrix} \\ &= \mathcal{H}_1 \bigoplus \mathcal{H}_2. \end{aligned} \tag{S22}$$

We find that the states $\Phi_\pm^\pm$ are not eigenmodes of the atomic cavity. In other words, the two reflection channels are not independent. The waveguide-mediated dissipative couplings mix these two channels. Owing to the dissipative couplings, the effective cavity supermodes can be created. An important feature of $H_{\rm c}$ is that two non-Hermitian Hamiltonians $\mathcal{H}_1$ and $\mathcal{H}_2$ are protected by anti-$\mathcal{PT}$ symmetry $(\mathcal{PT})\mathcal{H}_i(\mathcal{PT})^{-1} = -\mathcal{H}_i$. Therefore, *the emergence of cavity supermodes in the atom-dimer cavity is related to non-Hermitian phase transitions.*

In these two anti-$\mathcal{PT}$ symmetric Hamiltonians, $\mathcal{H}_1$ and $\mathcal{H}_2$, the non-Hermitian phase transitions do not require to tune the frequencies of the atoms. In the literature, anti-$\mathcal{PT}$ symmetry has been broadly studied, e.g., Refs. [50-58] in the main text. In previous works involving anti-$\mathcal{PT}$ symmetric systems, manipulations of non-Hermitian phase transitions relied on controlling the frequency detunings of resonators or atoms, depending on specific systems. Here, we show an atom-dimer proposal to realize anti-$\mathcal{PT}$-symmetry-protected non-Hermitian Hamiltonians.

A significant difference from anti-$\mathcal{PT}$ non-Hermitian systems studied in other works is that here the atomic coupling replaces the frequency detuning. Therefore, we are able to realize anti-$\mathcal{PT}$ phase transitions by adjusting the atomic coupling. Our scheme has two-fold advantages:

FIG. S5. Tuning anti-$\mathcal{PT}$ phase transitions of the atom-dimer cavity by means of the width $W = 2(\Omega + \Gamma)$ between the two reflection peaks of atomic mirrors. (a) Energy levels of the supermodes of the atom-dimer cavity. The second-order exceptional points are created at $W = \pm 4\Gamma$ and $W = 0$. (b) Decay rates of cavity supermodes. The degenerate supermodes have different decay rates in anti-$\mathcal{PT}$ symmetric phases, i.e., $W \in (-4\Gamma, 0) \cup (0, 4\Gamma)$.

(1) Changing frequency detuning would modify the waveguide-induced couplings between atoms in a waveguide. By tuning anti-$\mathcal{PT}$ phase transitions with atomic couplings, we are able to avoid waveguide-induced frequency-dependent couplings.
(2) As we demonstrated in Sec. (I), the coupling of two atoms gives rise to a nontrivial photon reflection. By studying how the atom-dimer cavity changes with atomic couplings, we can reveal the relation between the cavity and mirrors.

Because Hamiltonians $\mathcal{H}_1$ and $\mathcal{H}_2$ are protected by anti-$\mathcal{PT}$ symmetry, we can further diagonalize the atom-dimer cavity Hamiltonian Eq. (S22) as $H_c = \sum_j E_j |\Psi_j^R\rangle\langle\Psi_j^L|$, with $\langle\Psi_j^L|\Psi_{j'}^R\rangle = \delta_{jj'}$. The real and imaginary parts of the non-Hermitian energy spectrum E_j are shown in Fig. S5(a) and Fig. S5(b), respectively. There are four supermodes in the system. We use $\Psi_\pm$ to represent the two degenerate cavity supermodes in the anti-$\mathcal{PT}$ symmetric phases. Besides, there are two supermodes which are not protected by the anti-$\mathcal{PT}$ symmetry. These unprotected supermodes have energies different from $\Psi_\pm$. For $0 < W < 4\Gamma$ ($-4\Gamma < W < 0$), $\mathcal{H}_1$ ($\mathcal{H}_2$) has preserved the anti-$\mathcal{PT}$ symmetry. For simplicity, we only show two degenerate supermodes in the anti-$\mathcal{PT}$ symmetric phases of the main text.

The emergence of degenerate supermodes is related to mirror reflection. From Eq. (2) in the main text, we have

$$r_0\Omega^2 - 2\Gamma(1 - r_0)\Omega - 2\Gamma^2(1 - r_0) = 0, \tag{S23}$$

with $r_0 = \sqrt{R^{(0)}}$. By solving the above equation, we obtain

$$\Omega_1 = \frac{1 - r_0 - t_0}{r_0}\Gamma, \tag{S24}$$

$$\Omega_2 = \frac{1 - r_0 + t_0}{r_0}\Gamma, \tag{S25}$$

with $t_0 = \sqrt{1 - R^{(0)}}$. We can find that $-\Gamma \le \Omega_1 < 0$ and $\Omega_2 > 0$. The parameter regimes $-\Gamma < \Omega_1 < 0$ and $\Omega_2 > 0$ correspond to single-peak and two-peak mirrors, respectively. In Fig. S6(a), we show the energy levels and decay rates of supermodes in the cavity with single-peak mirrors. $R^{(0)} = 0$ corresponds to $\Omega_1 = -\Gamma$, i.e., no reflection is produced. Substituting Eq. (S25) to Eq. (6) in the main text, we can obtain Fig. S6(b), i.e., Fig. 2(d) in the main text. A reflection threshold of two-peak mirrors is found at $\Omega_2 = \Gamma$ for the emergence of cavity supermodes.

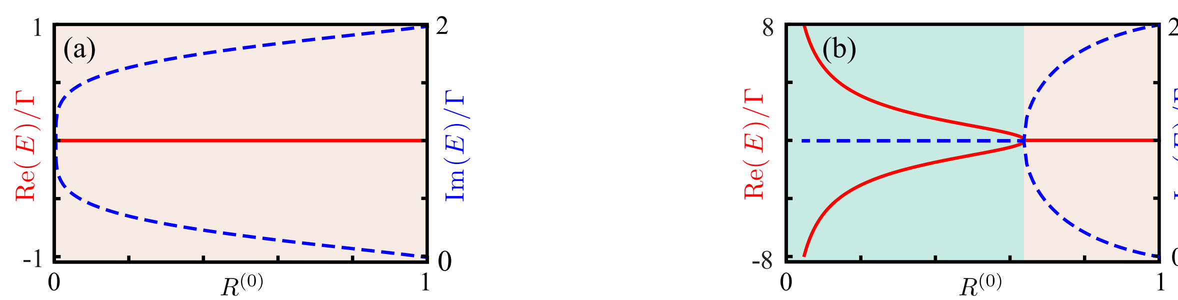

FIG. S6. Energy levels and decay rates of cavity supermodes changed by mirror reflection. Supermodes in the atom-dimer cavity with (a) single-peak mirrors and (b) two-peak mirrors.

B. Single-photon transmission of the atom-dimer cavity

The optical properties of a cavity are different from those of a waveguide. An important issue about the atom-dimer cavity is: how the output changes when mirror reflection varies. To answer this question, we start from the original Hamiltonian of the waveguide-cavity system

$$\begin{aligned} H = & \sum_{i=1}^{4} \omega_0 \sigma_i^+ \sigma_i^- + \Omega(\sigma_1^+ \sigma_2^- + \sigma_3^+ \sigma_4^- + \text{H.c.}) + ic \int dx \Big(\hat{a}_l^\dagger(x) \frac{\partial \hat{a}_l(x)}{\partial x} - \hat{a}_r^\dagger(x) \frac{\partial \hat{a}_r(x)}{\partial x} \Big) \\ & - g \sum_i \big(\sigma_i^+ \hat{a}_l(x_i) + \sigma_i^+ \hat{a}_r(x_i) + \text{H.c.} \big) + \varepsilon \sqrt{\Gamma c} \sum_i \big(\sigma_i^+ e^{ik_{\text{in}} x_i - i\omega_{\text{in}} t} + \text{H.c.} \big). \end{aligned} \tag{S26}$$

Here, $\hat{a}_{l,r}$ ($\hat{a}_{l,r}^\dagger$) are the annihilation (creation) operators for the left and right propagating photons; g denotes the coupling between atoms and photons in the waveguide; x_i is the position of the ith atom along the waveguide; and ε is assumed to be a classical coherent field. The continuous photonic modes make the waveguide act as a reservoir. Considering the Born-Markov approximation, we trace out the photonic degrees of freedom, and obtain the master equation for the atomic operators

$$\dot{\rho} = -i(H_{\text{eff}} \rho - \rho H_{\text{eff}}^\dagger) + 2\Gamma \sum_{ij} \sigma_i^- \rho \sigma_j^+. \tag{S27}$$

Within the rotating-wave approximation, and in the rotating frame with respect to the probe field frequency, the effective non-Hermitian Hamiltonian is

$$\begin{aligned} H_{\text{eff}} = & - \sum_i \Delta \sigma_i^+ \sigma_i^- + \Omega(\sigma_1^+ \sigma_2^- + \sigma_3^+ \sigma_4^- + \text{H.c.}) - i\Gamma \sum_{i,j} e^{ik_0|x_i - x_j|} \sigma_i^+ \sigma_j^- \\ & + \varepsilon \sqrt{\Gamma c} \sum_i \big(\sigma_i^+ e^{ik_{\text{in}} x_i} + \text{H.c.} \big). \end{aligned} \tag{S28}$$

with $\Delta = c(k_{\text{in}} - k_0)$ and $k_0 = \omega_0 / c$. The dynamics of the system is captured by

$$\langle \dot{\sigma}_i^- \rangle = i\Delta \langle \sigma_i^- \rangle - i\Omega \langle \sigma_{i+(-1)^{i-1}}^- \rangle - \Gamma \sum_j \langle \sigma_j^- \rangle e^{ik_0 |x_i - x_j|} - i\varepsilon \sqrt{\Gamma c} e^{ik_{\text{in}} x_i}. \tag{S29}$$

From the input-output method [S7], the transmitted field is

$$\hat{a}_t(x) = \varepsilon e^{ik_{\text{in}} x} - i \sum_i \sqrt{\frac{\Gamma}{c}} \sigma_i^- e^{ik_0(x - x_i)}. \tag{S30}$$

Therefore, the output field is dominated by the dynamics of atomic coherence, which is related to the direct coupling Ω and the waveguide-mediated coupling in [see Eq. (S29)]. From Eq. (S29), we can obtain the steady-state solution of the atomic coherence

$$\langle \boldsymbol{\sigma}^- \rangle = \varepsilon \sqrt{\Gamma c} (\Delta - H_c)^{-1} \boldsymbol{V}, \tag{S31}$$

with $\langle \boldsymbol{\sigma}^- \rangle = (\langle \sigma_1^- \rangle, \langle \sigma_2^- \rangle, \langle \sigma_3^- \rangle, \langle \sigma_4^- \rangle)^\top$ and $\boldsymbol{V} = (e^{ik_0 x_1}, e^{ik_0 x_2}, e^{ik_0 x_3}, e^{ik_0 x_4})^\top$. The cavity Hamiltonian H_c is shown in Eq. (S18). We have assumed that $|k_{\text{in}} - k_0| d \ll 1$. In terms of the biorthogonal basis of the non-Hermitian cavity Hamiltonian H_c, we have

$$\langle \boldsymbol{\sigma}^- \rangle = \varepsilon \sqrt{\Gamma c} \sum_j \frac{|\Psi_j^R\rangle \langle \Psi_j^L|}{\Delta - \text{Re}(E_j) - i\text{Im}(E_j)} \boldsymbol{V}. \tag{S32}$$

From Eq. (S30), we have the photon transmission amplitude

$$\begin{aligned} t &= \frac{\langle \hat{a}_t(x) \rangle}{\varepsilon e^{ik_{\text{in}} x}} \\ &= 1 - i\Gamma \sum_j \frac{\boldsymbol{V}^\dagger |\Psi_j^R\rangle \langle \Psi_j^L| \boldsymbol{V}}{\Delta - \text{Re}(E_j) - i\text{Im}(E_j)}. \end{aligned} \tag{S33}$$

This formula allows us to study the role played by cavity supermodes in producing the output field. In the waveguide with a single atom, the photon transmission amplitude is

$$t = 1 - \frac{i\Gamma}{\Delta + i\Gamma}. \tag{S34}$$

It comes from two contributions: the incident photon in the waveguide and the photon scattered by the atom. The superposition of these two components produces vanishing transmission at resonance ($\Delta = 0$). Namely, a single atom gives rise to complete photon reflection in a waveguide. Therefore, it acts as a mirror. For waveguide QED with many atoms, the transmission amplitude is determined by all eigenmodes of the system [see Eq. (S33)]. As we studied in Ref. [S2], subradiant states are responsible for reduced photon transmission, in agreement with the single-atom scattering. However, the slow-decay supermode Ψ_- in the atom-dimer cavity produces an anomalous transmission peak. This enhanced photon transmission effect reveals the cavity-like photon transport of the slow-decay supermode.

In cavity QED, the photon transmission exhibits a Lorentzian peak, where the linewidth is the decay rate of the cavity mode [S8]. The cavity-like optical feature of the atom-dimer cavity is not solely attributed to the slow-decay supermode. The supermode Ψ_+ plays an important role. At $\Omega = 0$, the atom-dimer cavity gives rise to a transmissionless spectrum owing to anti-Bragg scattering in atomic mirrors. The supermode Ψ_- does not scatter photons because it decouples with the waveguide, i.e., $\Gamma_- = 0$. So, the transmissionless spectrum is produced by dissipative supermodes in the atom-dimer cavity. From Fig. S5, we know that the fast-decay supermode Ψ_+ is responsible for the transmissionless photon transport around $\Delta = 0$. For a small atomic coupling $\Omega \ll \Gamma$, optical responses of those dissipative supermodes which are responsible for photon transport at $\Omega = 0$ are not changed too much. Quantum interference between scattered photons from these supermodes yields vanishing transmission. However, the slow-decay supermode Ψ_- couples to the waveguide, leading to the net effect of photon transmission

$$t \approx \frac{\Gamma_-}{i\Delta + \Gamma_-}. \tag{S35}$$

As a result, the incident photon can transmit through the atom-dimer cavity at resonance ($\Delta = 0$). Equation (S35) is the photon transmission of the bare optical cavities [S8], with decay rate Γ_- of the cavity mode. This is evidence that the slow-decay supermode Ψ_- plays the role of cavity mode. Therefore, the slow- and fast-decay supermodes in the atom-dimer cavity give rise to a cavity-like optical response. This cavity-like photon transport is crucial for observing interesting quantum phenomena arising from non-Hermitian cavity-atom coupling.

C. Atom-dimer cavity without anti-$\mathcal{PT}$ symmetry protection

In the main text, we show that the atom-dimer cavity is protected by the anti-$\mathcal{PT}$ symmetry. This symmetry protection comes from the special cavity structure shown in Fig. S4(a). There are two conditions to realize the atom-dimer cavity: (1) The atom-dimer mirrors should obey the anti-Bragg condition; (2) The distance between two atomic mirrors should be $n\lambda_0/2$ with n being an integer. However, in experiments, the distance between atoms might deviate from these values. Therefore, the anti-$\mathcal{PT}$ symmetry can be broken. In Figs. S7(a) and S7(b), we show cavity structures where these two conditions are not satisfied. In the following, we discuss how the atomic cavity is changed when these two conditions are not met.

At first, we consider atom-dimer mirrors that do not satisfy the anti-Bragg condition. We assume that the distance between two atoms in a mirror is $(\lambda_0/4 + \Delta d)$ with $\Delta d \ll \lambda_0$. From the waveguide-induced couplings Eqs. (S3) and

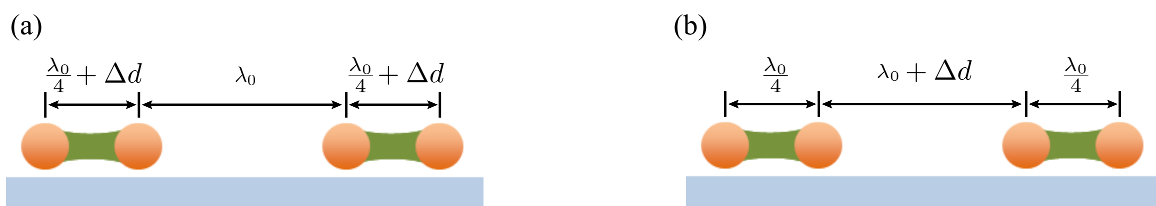

FIG. S7. Atom-dimer cavity without satisfying anti-PT symmetry. (a) The distance between two mirrors is $\lambda_0 + \Delta d$. (b) The distance between atoms in atom-dimer mirrors is $(\lambda_0/4 + \Delta d)$. We assume that $\Delta d \ll \lambda_0$.

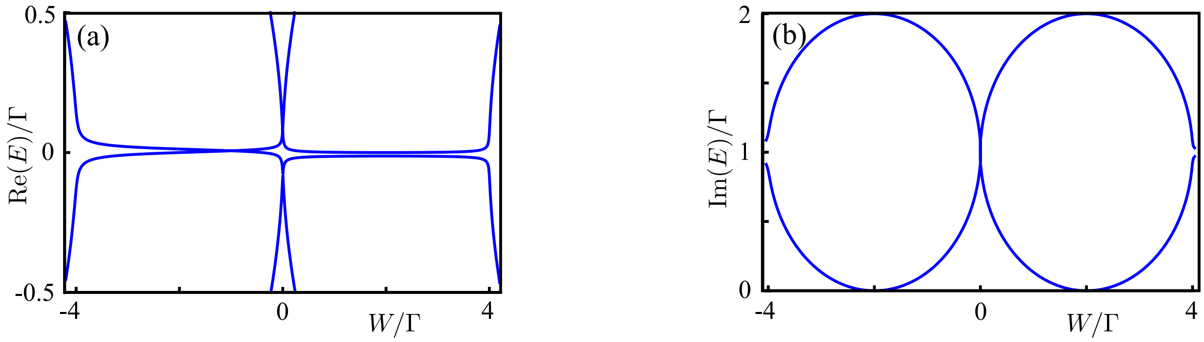

FIG. S8. (a) Energy spectrum of the atomic cavity with a distance $(\lambda_0 + \Delta d)$ between the two mirrors. (b) Decay rates of two cavity supermodes. We consider $\Delta d = 0.001\lambda_0$.

(S4), we obtain the effective coupling between two atoms in a mirror

$$\begin{aligned} g_{12} - i\gamma_{12} &= \Gamma \sin\left(\frac{\pi}{2} + \frac{2\pi\Delta d}{\lambda_0}\right) - i\Gamma\cos\left(\frac{\pi}{2} + \frac{2\pi\Delta d}{\lambda_0}\right) \\ &\approx \Gamma - i\Gamma\delta, \end{aligned} \tag{S36}$$

with $\delta = 2\pi\Delta d/\lambda_0$. Obviously, deviation from the anti-Bragg condition introduces dissipative coupling to two mirror atoms. Similarly, we can calculate the couplings between atoms in two mirrors. Therefore, the Hamiltonian of the atomic cavity becomes

$$H_{\rm c}^{'} \approx \begin{pmatrix} -i\Gamma & \Omega+\Gamma-i\Gamma\delta & \Gamma-i\Gamma\delta & -2\Gamma\delta+i\Gamma \\ \Omega+\Gamma-i\Gamma\delta & -i\Gamma & -i\Gamma & \Gamma-i\Gamma\delta \\ \Gamma-i\Gamma\delta & -i\Gamma & -i\Gamma & \Omega+\Gamma-i\Gamma\delta \\ -2\Gamma\delta+i\Gamma & \Gamma-i\Gamma\delta & \Omega+\Gamma-i\Gamma\delta & -i\Gamma \end{pmatrix}. \tag{S37}$$

After making the transformation U in Eq. (S21), we obtain

$$\begin{aligned} H_{\rm c}^{'} &= \begin{pmatrix} \Gamma\delta-\Omega-i\Gamma & \Gamma\delta-i\Gamma & 0 & 0 \\ \Gamma\delta-i\Gamma & \Gamma\delta+\Omega-i\Gamma & 0 & 0 \\ 0 & 0 & -\Omega-2\Gamma-\Gamma\delta-i(\Gamma-2\Gamma\delta) & -\Gamma\delta+i\Gamma \\ 0 & 0 & -\Gamma\delta+i\Gamma & \Omega+2\Gamma-\Gamma\delta-i(\Gamma+2\Gamma\delta) \end{pmatrix} \\ &= \mathcal{H}_1^{'} \bigoplus \mathcal{H}_2^{'}. \end{aligned} \tag{S38}$$

We can find that, because of the nonzero parameter δ, $\mathcal{H}_1^{'}$ and $\mathcal{H}_2^{'}$ do not preserve the anti-$\mathcal{PT}$ symmetry. In Figs. S8(a) and S8(b), we show the energy spectrum and decay rates of two cavity supermodes, respectively. Due to symmetry breaking induced by δ, the two supermodes are not degenerate. The energy spectrum for $W > 0$ is different from the one for $W < 0$. For $W > 0$, the energy spectrum is split. However, for $W < 0$, the two energy levels cross each other. This means that the dispersive coupling is important for an atom-dimer mirror. The decay rates of these two supermodes are almost unchanged.

Now we study that the distance between two atomic mirrors deviates from λ_0 by Δd, as shown in Fig. S7(b). The coupling between two middle atoms is

$$\begin{aligned} g_{23} - i\gamma_{23} &= \Gamma \sin\left(\frac{2\pi\Delta d}{\lambda_0}\right) - i\Gamma\cos\left(\frac{2\pi\Delta d}{\lambda_0}\right) \\ &\approx \Gamma\delta - i\Gamma, \end{aligned} \tag{S39}$$

i.e., a weak dispersive coupling is introduced. We can calculate couplings between other atoms in two mirrors. The Hamiltonian of the cavity becomes

$$\tilde{H}_{\rm c} = \begin{pmatrix} -i\Gamma & \Omega+\Gamma & \Gamma-i\Gamma\delta & -\Gamma\delta+i\Gamma \\ \Omega+\Gamma & -i\Gamma & \Gamma\delta-i\Gamma & \Gamma-i\Gamma\delta \\ \Gamma-i\Gamma\delta & \Gamma\delta-i\Gamma & -i\Gamma & \Omega+\Gamma \\ -\Gamma\delta+i\Gamma & \Gamma-i\Gamma\delta & \Omega+\Gamma & -i\Gamma \end{pmatrix}. \tag{S40}$$

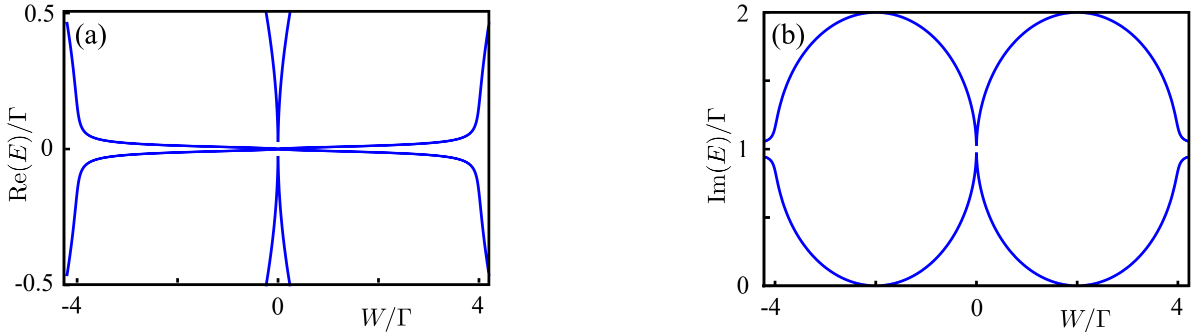

FIG. S9. (a) Energy spectrum of the atomic cavity where the distance between two mirrors is $(\lambda_0 + \Delta d)$. (b) Decay rates of two cavity supermodes. We consider $\Delta d = 0.001\lambda_0$.

The slight change of distance between the two mirrors alters the couplings between these two mirrors, i.e., the second and third terms in Eq. (S20). Similarly, the transformation U in Eq. (S21) simplifies the cavity Hamiltonian as

$$\begin{aligned}\tilde{H}_{\mathrm{c}} &= \begin{pmatrix} -\Omega - i(\Gamma+\Gamma\delta) & \Gamma\delta - i\Gamma & 0 & 0 \\ \Gamma\delta - i\Gamma & \Omega - i(\Gamma-\Gamma\delta) & 0 & 0 \\ 0 & 0 & -\Omega - 2\Gamma - i(\Gamma-\Gamma\delta) & -\Gamma\delta + i\Gamma \\ 0 & 0 & -\Gamma\delta + i\Gamma & \Omega + 2\Gamma - i(\Gamma+\Gamma\delta) \end{pmatrix} \\ &= \tilde{\mathcal{H}}_1 \bigoplus \tilde{\mathcal{H}}_2. \end{aligned} \tag{S41}$$

As shown in Fig. S9(a), the energy levels of two cavity supermodes $\Psi_\pm$ become split. Their decay rates are robust to the perturbation of cavity length shown in Fig. S9(b). Here, we consider $\Delta d = 0.001\lambda_0$. For superconducting artificial atoms with $\omega_0 = 5 \times 2\pi$ GHz, $0.001\lambda_0$ is about 60 μm. In experiments, the coupling points of artificial atoms in a waveguide can be controlled with high accuracy [S9] such that Δd can be much smaller than $0.001\lambda_0$.

In Fig. S10(a), we show the population dynamics of the probe atom for the atom-dimer cavity without obeying the anti-Bragg condition. Dark polaritons exist for $\Delta d = 0.001\lambda_0$ at different values of atomic coupling Ω. Hence, the state transfer between the probe atom and atom-dimer cavity is robust to the change of atomic spacing in mirror atoms. In Fig. S10(b), we consider that positions of the probe atom and atoms of the cavity have disorder $\tilde{x}_i = x_i + \Delta x_i$, with $i = 1, 2, 3, 4, 5$. Here, x_i represents the disorder-free atomic position of the ith atom, and $\Delta x_i \in [-\varepsilon\lambda_0, \varepsilon\lambda_0]$ denotes its disorder with strength ε. We find that even at large disorder strength, e.g., $\varepsilon = 0.01$, population of the probe atom exhibits long-lasting Rabi oscillations. This means that the dark polaritons are robust to disorder in the atomic position.

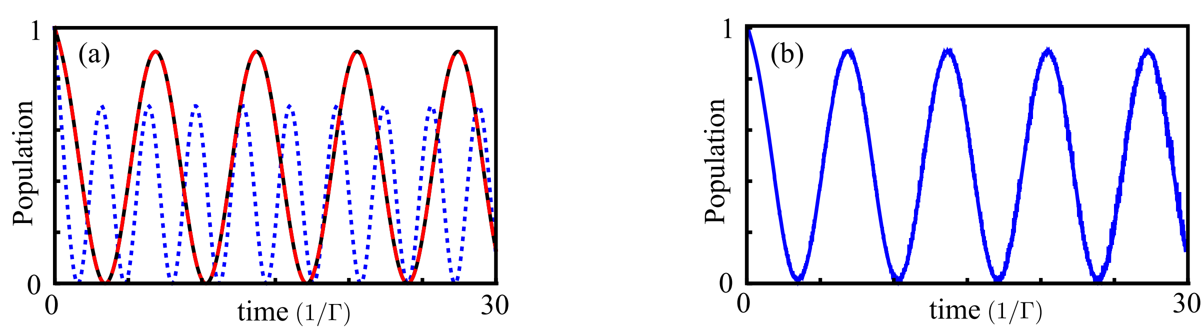

FIG. S10. (a) Population dynamics of the probe atom when the atom-dimer cavity does not meet the anti-Bragg condition. Black-solid and red-dashed curves correspond to $\Delta d = 0$ and $\Delta d = 0.001\lambda_0$, respectively, at $\Omega = \gamma = 0.1\Gamma$. The blue-dotted curve denotes $\Delta d = 0.001\lambda_0$ at $\Omega = \gamma = 0.4\Gamma$. (b) Population dynamics of the probe atom with atomic position $\tilde{x}_i = x_i + \Delta x_i$. Here, x_i denotes the atomic position without disorder, and $\Delta x_i \in [-\varepsilon\lambda_0, \varepsilon\lambda_0]$ with disorder strength ε. Here, we consider the disorder strength $\varepsilon = 0.01$ and $\Omega = \gamma = 0.1\Gamma$.

III. ATOM-DIMER CAVITY QED AND MIRROR-TUNED POLARITONS

According to cavity QED theory, a cavity which nontrivially modifies the distribution of electromagnetic fields can be detected with a probe atom. To study quantum optical phenomena produced by the atom-dimer cavity, we consider a probe atom in the cavity. The coupling between the probe atom and the atom-dimer cavity is mediated by continuous photonic modes in the waveguide. We assume that the decay rate of the probe atom in the waveguide is γ, different from the decay rate Γ of the mirror atoms. The atom-cavity interaction is described by

$$H_{\text{int}} = (\delta\omega - i\gamma)\sigma_p^+\sigma_p^- - i\sum_{j=1}^{4}\sqrt{\gamma\Gamma}e^{i\phi_j}(\sigma_j^+\sigma_p^- + \sigma_p^+\sigma_j^-), \tag{S42}$$

with a detuning $\delta\omega$ between the probe atom and mirror atoms, and $\phi_j = 2\pi|x_j - x_p|/\lambda_0$. In order to study the atom-dimer cavity QED, we should know how the probe atom interacts with the effective cavity mode. We rewrite the interaction Hamiltonian in terms of cavity supermodes

$$\begin{aligned} H_{\text{int}} &= \Big(|\psi_p\rangle\langle\psi_p| + \sum_j |\Psi_j^R\rangle\langle\Psi_j^L|\Big) H_{\text{int}} \Big(|\psi_p\rangle\langle\psi_p| + \sum_j |\Psi_j^R\rangle\langle\Psi_j^L|\Big) \\ &= (\delta\omega - i\gamma)|\psi_p\rangle\langle\psi_p| + \sum_j \langle\psi_p|H_{\text{int}}|\Psi_j^R\rangle|\psi_p\rangle\langle\Psi_j^L| + \sum_j \langle\Psi_j^L|H_{\text{int}}|\psi_p\rangle|\Psi_j^R\rangle\langle\psi_p|, \end{aligned} \tag{S43}$$

with $\langle\psi_p|H_{\text{int}}|\Psi_j^R\rangle = -i\sqrt{\gamma\Gamma}\sum_{j'} e^{i\phi_{j'}}\langle\psi_{j'}|\Psi_j^R\rangle$ and $\langle\Psi_j^L|H_{\text{int}}|\psi_p\rangle = -i\sqrt{\gamma\Gamma}\sum_{j'} e^{i\phi_{j'}}\langle\Psi_j^L|\psi_{j'}\rangle$. The couplings between the probe atom and two supermodes, which are not protected by the anti-$\mathcal{PT}$ symmetry, are denoted by $\tilde{G}_R = \langle\psi_p|H_{\text{int}}|\Psi_1^R\rangle$ and $\tilde{V}_R = \langle\psi_p|H_{\text{int}}|\Psi_4^R\rangle$, where 1 and 4 indicate supermodes with lower and upper energy levels, respectively. In Figs. S11(a) and S11(b), we show real and imaginary parts of $\tilde{G}_R$ and $\tilde{V}_R$, respectively. Different from the degenerate supermodes $\Psi_\pm$, these two unprotected supermodes have maximal couplings with the probe atom at the center or boundaries of the cavity. When the probe atom is placed at $x_p = \lambda_0/4$ or $x_p = 3\lambda_0/4$ in the cavity, it has a vanishing coupling with these two supermodes. Hence, we can study cavity QED produced by two degenerate cavity supermodes $\Psi_\pm$.

In cavity QED with single-atom mirrors, as studied in experiments [S6], the dark state (effective cavity mode) has a coherent coupling with the probe atom. This is similar to optical cavities where the probe atom is coherently coupled to a single cavity mode. Therefore, the coupling between the effective cavity mode and the probe atom gives rise to polaritons. However, the superradiant mode degenerate with the effective cavity mode is not coupled to the probe atom. The role played by the superradiant mode has not been discussed in Ref. [S6]. In the atom-dimer cavity we study in this work, the fast-decay supermode (superradiant mode) is degenerate with the effective cavity mode. Naively, the role played by the fast-decay supermode might appear to be negative. However, this is not the case.

In the atom-dimer cavity protected by the anti-$\mathcal{PT}$ symmetry, both slow- and fast-decay supermodes are coupled to the probe atom. In terms of two supermodes $\Psi_\pm$, the Hamiltonian for the cavity-atom system can be written as

$$\tilde{H} = \begin{pmatrix} -i\Gamma_- & 0 & G_L \\ 0 & -i\Gamma_+ & V_L \\ G_R & V_R & \delta\omega - i\gamma \end{pmatrix}, \tag{S44}$$

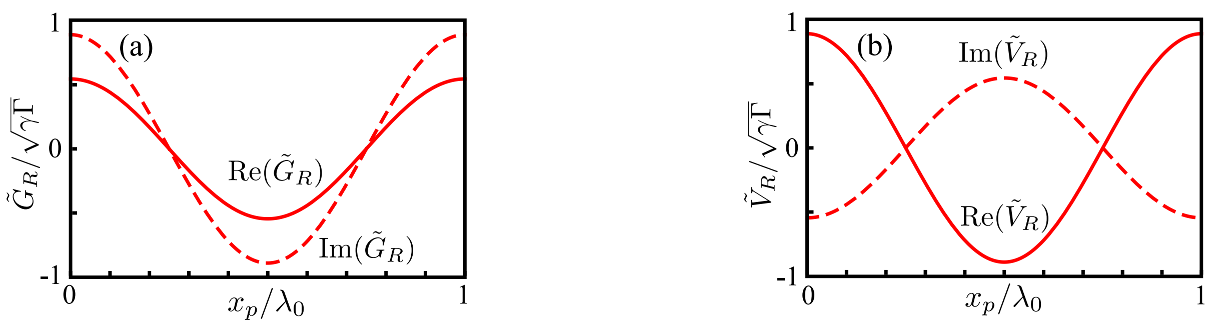

FIG. S11. (a, b) Couplings between the probe atom and two supermodes which are not protected by the anti-$\mathcal{PT}$ symmetry. Solid and dashed curves correspond to coherent and dissipative couplings, respectively. Here, we consider $W = 2.4\Gamma$ and $\gamma = 0.2\Gamma$.

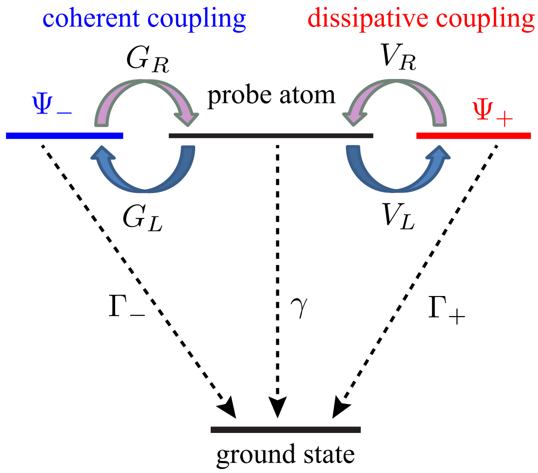

FIG. S12. Non-Hermitian couplings between the probe atom and the two degenerate cavity supermodes $\Psi_\pm$. The supermode Ψ_+ has large decay rate and is dissipatively coupled with the probe atom. The supermode Ψ_- with low decay rate has coherent non-Hermitian coupling with the probe atom.

where $G_{R,L}$ and $V_{R,L}$ are coherent and dissipative atom-cavity couplings, respectively. For clarity, we show these couplings in Fig. S12. The fast-decay supermode Ψ_+ has nonreciprocal dissipative couplings $V_{R,L}$ with the probe atom, and the coupling strengths are as large as the couplings $G_{R,L}$ between the slow-decay supermode Ψ_- and the probe atom. Specifically, in the anti-$\mathcal{PT}$-symmetry-protected regime, the couplings are $G_R = \sqrt{\gamma W}$, $V_R = iG_R$, $G_L = G_R/\sqrt{1-\Omega^2/\Gamma^2}$ and $V_L = V_R/\sqrt{1-\Omega^2/\Gamma^2}$. As we studied in the main text, G_R reveals the intrinsic relation between mirror reflection and cavity properties. Specifically, the coherent strong coupling in the cavity is related to the reflection threshold of atom-dimer mirrors.

To study the non-Hermitian physics produced by atom-cavity interactions, we calculate the eigenvalues of $|\tilde{H} - E| = 0$, i.e.,

$$E^3 + x_1 E^2 + x_2 E + x_3 = 0, \tag{S45}$$

with

$$x_1 = i(\Gamma_- + \Gamma_+ + \gamma), \tag{S46}$$
$$x_2 = -\gamma(\Gamma_- + \Gamma_+) - \Gamma_-\Gamma_+ - V_R V_L - G_R G_L, \tag{S47}$$
$$x_3 = -i\Gamma_- V_R V_L - i\Gamma_+ G_R G_L - i\gamma\Gamma_-\Gamma_+. \tag{S48}$$

We find $V_R V_L + G_R G_L = 0$ and $\Gamma_- V_R V_L + \Gamma_+ G_R G_L = 2\Gamma G_R^2$. In these coefficients x_i $(i = 1, 2, 3)$, only x_3 is related to G_R^2, which comes from both coherent and dissipative couplings. Therefore, it can be concluded that Eq. (S45) is determined by the coupling G_R. In other words, G_R characterizes the efficient atom-cavity coupling as we claimed in the main text. The cubic equation Eq. (S45) can be solved using Cardano's formula [S10]. By introducing $E = \mu - x_1/3$, we have

$$\mu^3 + p\mu + q = 0, \tag{S49}$$

with $p = x_2 - x_1^2/3$ and $q = x_3 - x_1 x_2/3 + 2x_1^3/27$. With

$$u = \left(-\frac{q}{2} + \sqrt{\frac{p^3}{27} + \frac{q^2}{4}}\right)^{1/3}, \tag{S50}$$

$$v = \left(-\frac{q}{2} - \sqrt{\frac{p^3}{27} + \frac{q^2}{4}}\right)^{1/3}, \tag{S51}$$

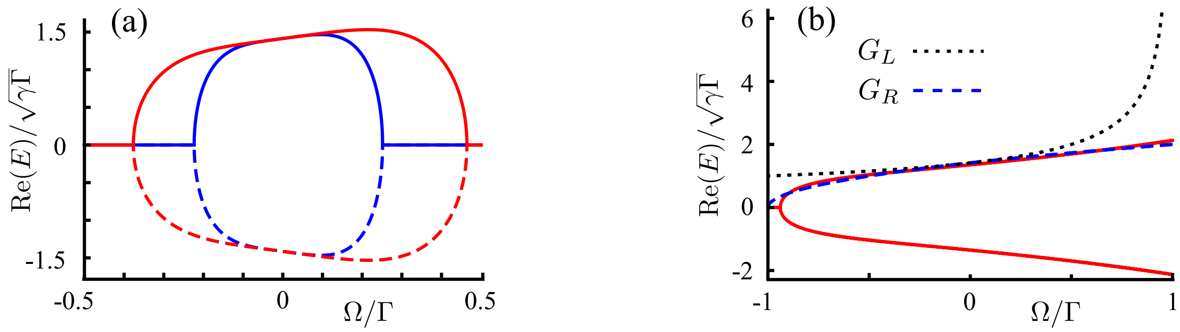

FIG. S13. (a) Cavity-atom polaritons in the coherent coupling regime. Blue-solid (red-solid) and blue-dashed (red-dashed) curves correspond to $\mathrm{Re}(E_1)$ and $\mathrm{Re}(E_2)$, respectively, for $\gamma = 0.0001\Gamma$ ($\gamma = 0.001\Gamma$). (b) Energy levels of the polaritons (red-solid) and couplings $G_{R,L}$ between the probe atom and the slow-decay supermode. Here, we consider $\gamma = 0.2\Gamma$.

we can analytically solve Eq. (S49). Therefore, the final solutions of Eq. (S45) are

$$E_1 = u + v - \frac{x_1}{3}, \tag{S52}$$

$$E_2 = \left(-\frac{1}{2} - i\frac{\sqrt{3}}{2}\right)u + \left(-\frac{1}{2} + i\frac{\sqrt{3}}{2}\right)v - \frac{x_1}{3}, \tag{S53}$$

$$E_3 = \left(-\frac{1}{2} + i\frac{\sqrt{3}}{2}\right)u + \left(-\frac{1}{2} - i\frac{\sqrt{3}}{2}\right)v - \frac{x_1}{3}. \tag{S54}$$

In these three solutions, there are two polaritons arising from coherent atom-cavity interactions, as shown in Fig. S12. In Fig. S13(a), we show the real parts of E_1 and E_2 when the probe atom is weakly coupled to the waveguide, i.e., $\gamma \ll \Gamma$. The large mirror reflection in the strong-coupling regime leads to efficient energy exchange between the probe atom and the supermode Ψ_-. The cavity-atom polaritons are formed due to cavity-enhanced interactions. This is the *coherent coupling regime* of cavity QED. The energies of the polaritons are not symmetric because the atom-cavity coupling is stronger in $\Omega > 0$ than $\Omega < 0$. When $|\Omega|$ is increased, the loss of the effective cavity mode Ψ_- becomes significant. The excitation in the probe atom is transported to two cavity supermodes and quickly dissipates to the waveguide. In other words, no coherent energy exchange takes place between the probe atom and the cavity. Therefore, the polaritons disappear in the *dissipative coupling regime*. In Fig. S13(b), we show energies of polaritons and coherent atom-cavity couplings $G_{R,L}$. We find that G_R agrees well with the polariton's energy. This justifies the role played by G_R in characterizing the atom-cavity interaction.

In Fig. (S12), the coherent and dissipative couplings play different roles in controlling the dynamics of the probe atom. At first, we focus on the dissipative coupling between the probe atom and the supermode Ψ_+. The dissipative coupling mixes the probe atom and the supermode Ψ_+, as shown in Fig. S14. The decay rates of the eigenstates are

$$\kappa_\pm = \frac{1}{2}\Big(\gamma + \Gamma_+ \pm \sqrt{(\gamma - \Gamma_+)^2 - 4V_R V_L}\Big). \tag{S55}$$

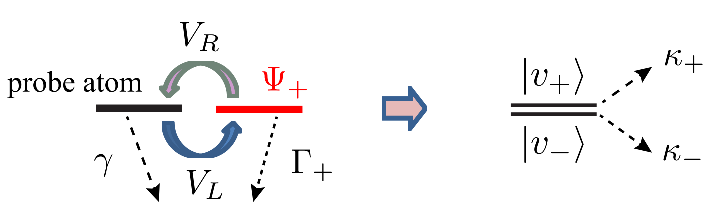

FIG. S14. Schematics of dissipatively coupled probe atom and fast-decay supermode Ψ_+. Two degenerate states $|v_\pm\rangle$ with decay rates $\kappa_\pm$ are produced.

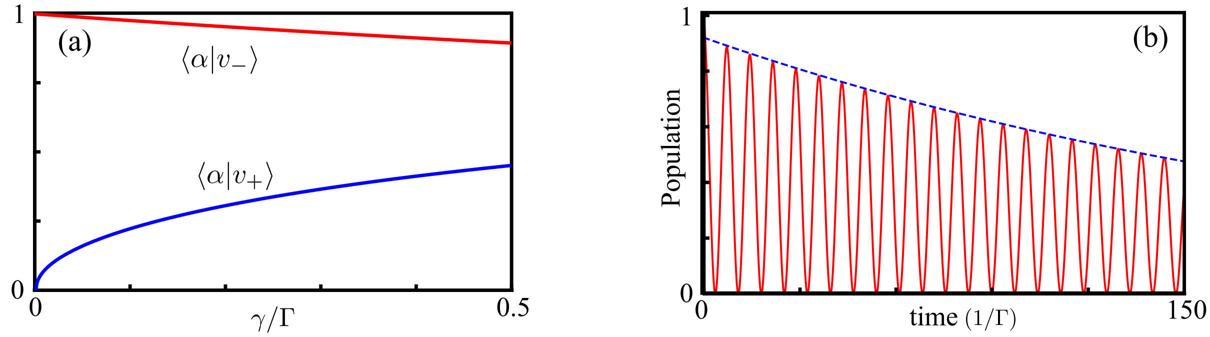

FIG. S15. (a) The component of the probe atom in $|v_\pm\rangle$. We consider $|\alpha\rangle = (1,0)^\top$. (b) Rabi oscillations (red-solid) of the probe atom for $\gamma = 0.1\Gamma$. The blue-dashed curve corresponds to a decay rate 0.0044Γ. Here, we consider $\Omega = 0$ for (a) and (b).

The eigenvectors are

$$|v_+\rangle = \frac{1}{\mathcal{N}_+}\begin{pmatrix} [-i\gamma + i\Gamma_+ - \sqrt{-(\gamma-\Gamma_+)^2 + 4V_RV_L}]/2V_R \\ 1 \end{pmatrix}, \tag{S56}$$

$$|v_-\rangle = \frac{1}{\mathcal{N}_-}\begin{pmatrix} [-i\gamma + i\Gamma_+ + \sqrt{-(\gamma-\Gamma_+)^2 + 4V_RV_L}]/2V_R \\ 1 \end{pmatrix}, \tag{S57}$$

where $\mathcal{N}_\pm$ are normalization factors. Here, $(1,0)^\top$ and $(0,1)^\top$ correspond to the probe atom and the supermode Ψ_+, respectively.

In Fig. S15(a), we plot the component of the probe atom in $|v_+\rangle$ and $|v_-\rangle$. The probe atom has large (small) component in $|v_-\rangle$ ($|v_+\rangle$). Without loss of generality, we consider that the decay rate of the probe atom is much smaller than in the mirror atoms, i.e., $\gamma \ll \Gamma$. The condition that $|v_-\rangle$ becomes a dark state ($\kappa_- = 0$) is $\gamma\Gamma_+ + V_RV_L = 0$, which gives rise to $\Omega = 0$.

We now consider the slow-decay supermode Ψ_-. Because of the large component of probe atom in $|v_-\rangle$, Ψ_- has coherent coupling with $|v_-\rangle$. This coupling is responsible for the energy splitting of polaritons, as shown in Fig. S13(a). At $\Omega = 0$, the supermode Ψ_- has vanishing decay rate. In other words, the states formed by the coupling between Ψ_- and $|v_-\rangle$ are dissipationless. However, taking into account the small coupling between Ψ_- and $|v_+\rangle$, we can obtain dissipative polaritons, which lead to slow-decaying Rabi oscillations.

In Fig. S15(b), we show the Rabi oscillations of the probe atom at $\Omega = 0$. From the period of the Rabi oscillations, we can obtain the coupling strength 0.44Γ, which agrees with the coupling $G_R = 0.447\Gamma$. The decay of the Rabi oscillations is 0.0044Γ, corresponding to a decay rate $\gamma_p = 0.0022\Gamma$ for the cavity-atom polaritons. Therefore, the dissipative coupling and coherent coupling play different roles in affecting the dynamics of the probe atom.

Figure S16(a) shows the transmission spectrum of the polaritons for $\Omega = 0$. The complete mirror reflection around $\Delta = 0$ makes polaritons invisible for $\delta\omega > 0$, similar to the cavity QED experiment with single-atom mirrors [S6]. By reducing the mirror reflection, *polaritons* can be observed in a broad range of parameter space. Spectroscopic measurement of polaritions in the atom-dimer cavity with two-peak mirrors has been studied in the main text. To compare with the results in experiment [S6], we consider atom-dimer mirrors with a single-peak reflection spectrum.

FIG. S16. Transmission for the coupled cavity-atom system at (a) $\Omega = 0$ and (b) $\Omega = -0.1\Gamma$. We assume that the probe atom has a waveguide-induced decay rate $\gamma = 0.1\Gamma$ and a free-space loss $\gamma' = 0.01\Gamma$.

In Fig. S16(b), we show the transmission spectrum of polaritons in the atom-dimer cavity with atomic coupling $\Omega = -0.1\Gamma$ between the mirror atoms. The cavity-like photon transport makes the polaritons detectable from photon transmission in the waveguide.

The solutions Eqs. (S52 – S54) can be simplified by considering $\Omega = \gamma$. Hence, we have $x_3 = x_1 x_2$. Therefore, Eq. (S45) can be written as

$$(E + x_1)(E^2 + x_2) = 0. \tag{S58}$$

This gives rise to three solutions

$$E_1 = \sqrt{\Omega^2 + 2\Gamma\gamma}, \tag{S59}$$

$$E_2 = -\sqrt{\Omega^2 + 2\Gamma\gamma}, \tag{S60}$$

$$E_3 = -i(2\Gamma + \gamma). \tag{S61}$$

Here, $E_{1,2}$ denote two *dark polaritons*, and E_3 contains the whole *dissipation* of the cavity-atom system. The fast-decay supermode nontrivially modifies the dissipation of the cavity-atom polaritons in the coherent coupling regime, and makes the atom-dimer cavity distinct from conventional single-mode optical cavities.

[S1] T. Shi, D. E. Chang, and J. I. Cirac, *Multiphoton-scattering theory and generalized master equations,* Phys. Rev. A **92**, 053834 (2015).

[S2] W. Nie, T. Shi, F. Nori, and Y.-X. Liu, *Topology-Enhanced Nonreciprocal Scattering and Photon Absorption in a Waveguide,* Phys. Rev. Appl. **15**, 044041 (2021).

[S3] D. E. Chang, L. Jiang, A. Gorshkov, and H. Kimble, *Cavity QED with atomic mirrors,* New J. Phys. **14**, 063003 (2012).

[S4] B. Kannan, A. Almanakly, Y. Sung, A. Di Paolo, D. A. Rower, J. Braumüller, A. Melville, B. M. Niedzielski, A. Karamlou, K. Serniak, A. Vepsäläinen, M. E. Schwartz, J. L. Yoder, R. Winik, J. I.-J. Wang, T. P. Orlando, S. Gustavsson, J. A. Grover, and W. D. Oliver, *On-demand directional microwave photon emission using waveguide quantum electrodynamics,* Nat. Phys. **19**, 394 (2023).

[S5] Y. P. Zhong, H.-S. Chang, K. J. Satzinger, M.-H. Chou, A. Bienfait, C. R. Conner, É. Dumur, J. Grebel, G. A. Peairs, R. G. Povey, D. I. Schuster, and A. N. Cleland, *Violating Bell's inequality with remotely connected superconducting qubits,* Nat. Phys. **15**, 741 (2019).

[S6] M. Mirhosseini, E. Kim, X. Zhang, A. Sipahigil, P. B. Dieterle, A. J. Keller, A. Asenjo-Garcia, D. E. Chang, and O. Painter, *Cavity quantum electrodynamics with atom-like mirrors,* Nature **569**, 692 (2019).

[S7] T. Caneva, M. T. Manzoni, T. Shi, J. S. Douglas, J. I. Cirac, and D. E. Chang, *Quantum dynamics of propagating photons with strong interactions: a generalized input-output formalism,* New J. Phys. **17**, 113001 (2015).

[S8] D. Plankensteiner, C. Sommer, H. Ritsch, and C. Genes, *Cavity Antiresonance Spectroscopy of Dipole Coupled Subradiant Arrays,* Phys. Rev. Lett. **119**, 093601 (2017).

[S9] B. Kannan, M. J. Ruckriegel, D. L. Campbell, A. Frisk Kockum, J. Braumüller, D. K. Kim, M. Kjaergaard, P. Krantz, A. Melville, B. M. Niedzielski, A. Vepsäläinen, R. Winik, J. Yoder, F. Nori, T. P. Orlando, S. Gustavsson, and W. D. Oliver, *Waveguide quantum electrodynamics with superconducting artificial giant atoms,* Nature **583**, 775 (2020).

[S10] H. Jing, Ş. K. Özdemir, H. Lü, and F. Nori, *High-order exceptional points in optomechanics,* Sci. Rep. **7**, 3386 (2017).